Bioorganic & Medicinal Chemistry 19 (2011) 6069–6076

Contents lists available at SciVerse ScienceDirect

Bioorganic & Medicinal Chemistry

journal homepage: www.elsevier.com/locate/bmc

Metronidazole acid acyl sulfonamide: A novel class of anticancer agents and potential EGFR tyrosine kinase inhibitors

Yin Luo [a], Yao Li [a], Ke-Ming Qiu [a], Xiang Lu [a], Jie Fu [b], Hai-Liang Zhu [a,*]

[a] State Key Laboratory of Pharmaceutical Biotechnology, Nanjing University, Nanjing 210093, People's Republic of China
[b] State Key Laboratory of Pollution Control & Resource Reuse, Nanjing University (Xianlin Campus), Nanjing 210046, People's Republic of China

ARTICLE INFO

Article history:
Received 14 July 2011
Revised 18 August 2011
Accepted 18 August 2011
Available online 26 August 2011

Keywords:
Metronidazole
Sulfonamide
EGFR
Antiproliferative activity
Molecular docking

ABSTRACT

A series of novel metronidazole derivatives were recently reported as potent anticancer agents targeting EGFR and HER-2 by our group [Qian, Y.; Zhang, H. J.; Zhang, H.; Xu, C.; Zhao, J.; Zhu, H. L. *Bioorg. Med. Chem.* **2010**, *18*, 4991]. Based on the previous results, we designed and synthesized a new series of metronidazole acid acyl sulfonamide derivatives and a new series of phenylacetyl benzenesulfonamide derivatives and their anticancer activities were evaluated as potential EGFR and HER-2 kinase inhibitors. Among all the compounds, compound **12** displayed the most potent inhibitory activity EGFR and HER-2 (IC_{50} = 0.39 μM for EGFR and IC_{50} = 1.53 μM for HER-2) and it also showed the most potent growth inhibitory activity against A549 and B16-F10 cancer cell line in vitro, with an IC_{50} value of 1.26 μg/mL for A549 and 0.35 μg/mL for B16-F10. Docking simulation was further performed to position compound **12** into the EGFR active site to determine the probable binding model.

1. Introduction

Epidermal growth factor receptor (EGFR) is a kind of tyrosine kinase firstly reported in the literature.[2,3] It has become one of the targets of anticancer drug research and development because of its widely distribution in the cell and important role in cell life. EGFRs are distributed in mammalian epithelial cell membranes and have relationships with cell proliferation, death, and differentiation. They are junctions to deliver extracellular growth signals intracellular. EGFR family comprise four members, including: EGFR (HER1/ErbB-1), ErbB-2 (HER2/neu), ErbB-3 (HER3), and ErbB-4 (HER4).[4] EGFR tyrosine kinase-mediated cell growth signaling pathway plays an important role in the formation and development of many types of solid tumors, such as non small cell lung cancer,[5] head and neck cancer,[6] and glioblastomas.[7] Overexpression of EGFR family receptors have always been observed in these tumors, approximately in 60% of all tumors.[5] EGFR and ErbB-2 are the hottest targets in current research and their overexpression or abnormal activation often cause cell malignant transformation. Also they have relationship with postoperative adverse, radiotherapy and chemotherapy resistance and tumor angiogenesis.[8]

In previous study, metronidazole (Fig. 1), a kind of nitroimidazole, has been selected as starting material for the preparation of 99mTc radiopharmaceuticals due to its affinity for hypoxic tumors.[9] On the mechanism level, nitroimidazole derivatives have attracted considerable attention as they showed a tendency to penetrate and accumulate in regions of tumors,[10–12] and can undergo bioreduction to yield electrophilic substances which can damage protein and nucleic acids.[13] Importantly, the toxicology and metabolism of nitroimidazoles, particularly metronidazole, have been characterized.[14,15] Therefore, nitroimidazoles may provide the attractive possibility of employing these molecules as carriers for targeted delivery in cancer therapy.[12,16] Based on the results, a series of novel metronidazole derivatives were recently reported as potent anticancer agents targeting EGFR and HER-2 in our group and compound **3h** (Fig. 1) was the most active agent with IC_{50} value of 0.62 μM for EGFR and 2.15 μM for HER-2.[4]

In addition, many acyl sulfonamides displayed potent biological activities and low toxicities in previous reports. Among them, some compounds showed their anticancer effects by inhibiting vascular endothelial growth factor receptor (VEGFR), such as compound **1** and **2** shown in Figure 1.[17] The two compounds had curative activity against colon adenocarcinoma, human colon, human prostate, and human breast cancer lines.[18] All of these encouraged us to continuously design and screen new metronidazole acyl sulfonamides as potential EGFR inhibition agents.

In this paper, the metronidazole derivatives were further combined with sulfonamides by amide bond, which was usually used to connect substructures in our laboratory. Meanwhile, we also synthesized the analogs (phenylacetyl benzenesulfonamide derivatives) of compound **1** and **2** to contrast with metronidazole derivatives because phenylacetic acid and metronidazole had the same length of side chain. The two series of compounds, metronidazole

* Corresponding author. Tel./fax: +86 25 83592672.
E-mail address: zhuhl@nju.edu.cn (H.-L. Zhu).

0968-0896/$ - see front matter © 2011 Elsevier Ltd. All rights reserved.
doi:10.1016/j.bmc.2011.08.038

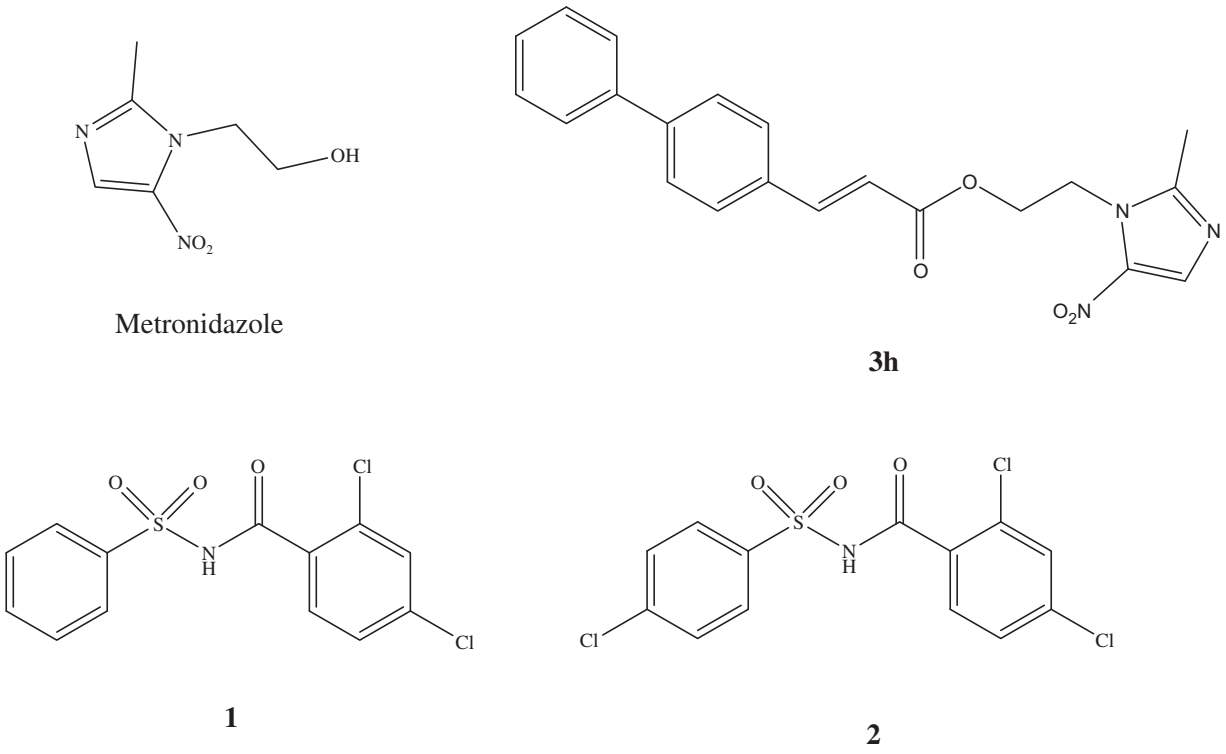

Figure 1. Chemical structures of some reported compounds.

acid benzenesulfonamide and phenylacetyl benzenesulfonamide derivatives, might exhibit synergistic effect in anticancer activities. The objectives of present work are to synthesize new acyl benzenesulfonamides; to evaluate their EGFR inhibition activities; to test their anticancer activities and to investigate the inhibitor interaction with EGFR by docking study.

2. Results and discussion

2.1. Chemistry

A series of novel metronidazole–sulfonamide derivatives (**10**–**14**) were synthesized by the routes outlined in Scheme 1. Compound **4** was synthesized from metronidazole (**3**) according to the modified procedure of Mirzaei et al.[19] Metronidazole was dissolved in water and sodium dichromate aqueous solution was added followed by drop wise addition sulfuric acid 50%. The mixture was stirred overnight and then neutralized. Compound **4** was obtained with yield of 65%. Then, synthesized compound **4**, active sulfonamides **5**–**9**, 4-dimethyaminopyridine (DMAP) and 1-[3-(dimethyamino)-propyl]-3-ethylcarbodiimide hydrochloride (EDCI) were dissolved in dichloromethane and refluxed overnight to give the desired compounds **10**–**14** (Table 1).

A series of novel phenylacetyl benzenesulfonamide derivatives (**20**–**44**) were also synthesized by the routes outlined in Scheme 2. Phenylacetic acids **15**–**19**, active sulfonamides **5**–**9**, DMAP and EDCI were dissolved in CH_2Cl_2 and refluxed to give the desired compounds **20**–**44**.

2.2. In vitro enzyme inhibition activity

The two series of benzenesulfonamide derivatives (**10**–**14** and **20**–**44**) were evaluated for their abilities to inhibit the autophosphorylation of EGFR kinases using a solid-phase ELISA assay. The inhibition constants (IC_{50}) of the compounds were summarized in Tables 2. It was observed that benzenesulfonamide derivatives

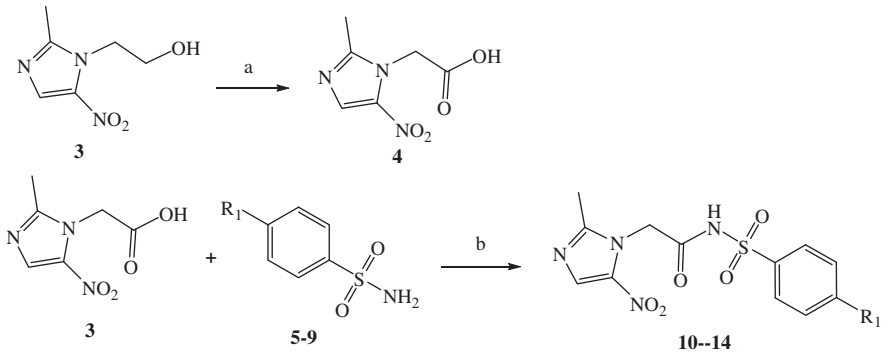

Scheme 1. General synthesis of sulfonamide derivatives (**10**–**14**). Reagents and conditions: (a) sodium dichromate, 50% sulfuric acid, 25 °C, overnight; (b) CH_2Cl_2, EDCI, DMAP, 25 °C, overnight.

Table 1
Chemical structures of benzenesulfonamide derivatives **10**–**14** and **20**–**44**

Compound	R_1	R_2	R_3	Compound	R_1	R_2	R_3
10	H	—	—	**30**	H	Br	H
11	CH_3	—	—	**31**	CH_3	Br	H
12	F	—	—	**32**	F	Br	H
13	Cl	—	—	**33**	Cl	Br	H
14	Br	—	—	**34**	Br	Br	H
20	H	F	H	**35**	H	OCH_3	H
21	CH_3	F	H	**36**	CH_3	OCH_3	H
22	F	F	H	**37**	F	OCH_3	H
23	Cl	F	H	**38**	Cl	OCH_3	H
24	Br	F	H	**39**	Br	OCH_3	H
25	H	Cl	H	**40**	H	H	Br
26	CH_3	Cl	H	**41**	CH_3	H	Br
27	F	Cl	H	**42**	F	H	Br
28	Cl	Cl	H	**43**	Cl	H	Br
29	Br	Cl	H	**44**	Br	H	Br

containing metronidazole skeleton (compounds **10**–**14**) showed fairly good inhibiting EGFR activities displaying IC_{50} values between 0.39 and 38.52 μM. The compounds with *para* halogen substituted (**12**–**14**) (IC_{50} = 0.39, 1.51, 2.17 μM for EGFR and IC_{50} = 1.53, 3.41, 3.59 μM for HER-2) exhibited significant inhibition activities in the order of fluorine > chlorine > bromine. Compound **11** with the electron donating substitute methyl had the lowest activity (IC_{50} = 3.43 μM). These results demonstrated that a hydrophobic and electron-withdrawing halogen group might have slightly promotion function to EGFR and HER-2 inhibition activities, however, electron donating substitutes had negative effects.

As illustrated in Table 2, compounds **20**–**44** displayed moderate EGFR inhibitory activities with IC_{50} ranging from 5.17 to 38.52 μM. In the case of constant B ring (Scheme 2) substituents, change of substituents on A ring can affect the activities of these compounds. Among the compounds **20**–**24**, these compounds with the halogen atom substituent (**22**–**24**) show stronger anticancer activity and the strength order is similar with A ring: fluorine > chlorine > bromine. Compounds **20** and **21** have the lowest activities. The explanation theory of B ring can be also applied on A ring. Compounds (**40**, IC_{50} = 24.68 μM for EGFR and IC_{50} = 26.33 μM for HER-2) with *meta*-substituted group showed slightly less potent activities than those of *para*-substituted (**30**, IC_{50} = 17.81 μM for EGFR and IC_{50} = 19.05 μM for HER-2).

Among all the compounds **22**–**44**, **22** (IC_{50} = 5.17 μM for EGFR and IC_{50} = 7.02 μM for HER-2) showed the best activity while the substituents in the A ring and B ring are both fluorine and fluorine atom is *para*-substituted in the A ring. The results showed that electron-withdrawing groups could enhance the activities of compounds. Compound **22** could be a promising lead for the further development of novel EGFR inhibition agents.

The above results indicated that the metronidazole skeleton in the benzenesulfonamide derivatives **10**–**14** might play an important role in the EGFR inhibitory activity which might be related with the electron-withdrawing nitro-group in metronidazole. This result was similar with the reported synthesized metronidazole derivatives[1] and conformed to our estimate. However, the metronidazole–benzenesulfonamide derivatives different with classical EGFR inhibitors (e.g., Gefitinib and Erlotinib) were reported EGFR inhibitors.

For the synthesized compounds, it was observed that the IC_{50} value for inhibiting HER-2 was higher than EGFR, however, they had the same trends. This might be attributed to the concentration of purified kinase HER-2 is higher than that of EGFR kinase in the experiments. Obviously, there was a reasonable correlation between sensitivities of EGFR and HER-2 to these synthesized compounds and this result was the same view that the highly homologous sequence of these two kinase catalytic domains decided their sensitivities.

2.3. Antiproliferative activity and molecular docking study

The in vitro anticancer activities of 10 compounds (**10**–**14** and **20**–**24**) with better inhibition activities against EGFR were tested using adenocarcinomic human alveolar basal epithelial cells

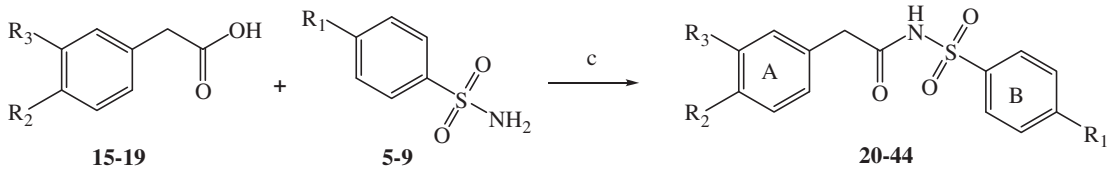

Scheme 2. General synthesis of sulfonamide derivatives (**20**–**44**). Reagents and conditions: (c) CH_2Cl_2, EDCI, DMAP, overnight.

Table 2
Inhibition activities of compounds **10**–**14** and **20**–**44** against EGFR and HER-2 (IC_{50}, μM)

Compounds	EGFR (μM)	HER-2 (μM)	Compounds	EGFR (μM)	HER-2 (μM)
10	2.94 ± 0.23	4.21 ± 0.35	**30**	17.81 ± 2.13	19.05 ± 1.57
11	3.43 ± 0.22	4.76 ± 0.42	**31**	18.35 ± 1.56	20.33 ± 1.78
12	0.39 ± 0.02	1.53 ± 0.18	**32**	14.53 ± 1.7	16.26 ± 1.38
13	1.51 ± 0.11	3.41 ± 0.32	**33**	15.92 ± 0.78	18.94 ± 1.93
14	2.17 ± 0.32	3.59 ± 0.28	**34**	17.26 ± 1.29	19.83 ± 1.56
20	6.74 ± 0.46	8.41 ± 0.76	**35**	26.2 ± 3.44	29.07 ± 3.02
21	8.28 ± 0.72	10.53 ± 1.41	**36**	38.52 ± 3.59	>50
22	5.17 ± 0.64	7.02 ± 0.65	**37**	21.84 ± 2.48	23.45 ± 2.38
23	5.93 ± 0.53	7.56 ± 0.82	**38**	32.85 ± 3.96	37.93 ± 3.15
24	6.41 ± 0.67	8.18 ± 0.94	**39**	24.15 ± 2.12	25.03 ± 2.04
25	11.91 ± 2.33	13.07 ± 1.24	**40**	24.68 ± 1.94	26.33 ± 2.92
26	13.73 ± 1.57	15.57 ± 1.63	**41**	26.17 ± 2.75	27.89 ± 2.46
27	9.59 ± 0.85	11.05 ± 1.09	**42**	18.72 ± 1.88	20.45 ± 1.65
28	10.34 ± 1.92	13.32 ± 1.46	**43**	21.28 ± 2.55	23.46 ± 2.47
29	11.29 ± 1.52	13.56 ± 1.47	**44**	24.33 ± 2.39	27.38 ± 2.33
Erlotinib	0.032 ± 0.002	0.16 ± 0.02			

Table 3
Antiproliferative activities and docking parameters of compounds **10**–**14** and **20**–**24**

Compounds	A549 (IC_{50}, μg/mL)	B16-F10 (IC_{50}, μg/mL)	Binding energy ΔGb (kcal/mol)
10	3.96 ± 0.34	2.93 ± 0.27	−12.56
11	4.38 ± 0.43	3.55 ± 0.36	−11.09
12	1.26 ± 0.16	0.35 ± 0.03	−14.14
13	2.47 ± 0.26	0.92 ± 0.08	−13.78
14	3.03 ± 0.37	2.37 ± 0.25	−13.04
20	10.11 ± 0.94	9.07 ± 0.94	−8.17
21	12.04 ± 1.36	9.94 ± 1.36	−7.95
22	5.64 ± 0.51	4.23 ± 0.45	−10.06
23	6.28 ± 0.67	6.36 ± 0.68	−9.34
24	7.94 ± 0.79	8.2 ± 0.92	−8.25
Erlotinib	0.13 ± 0.01	0.022 ± 0.001	−8.83

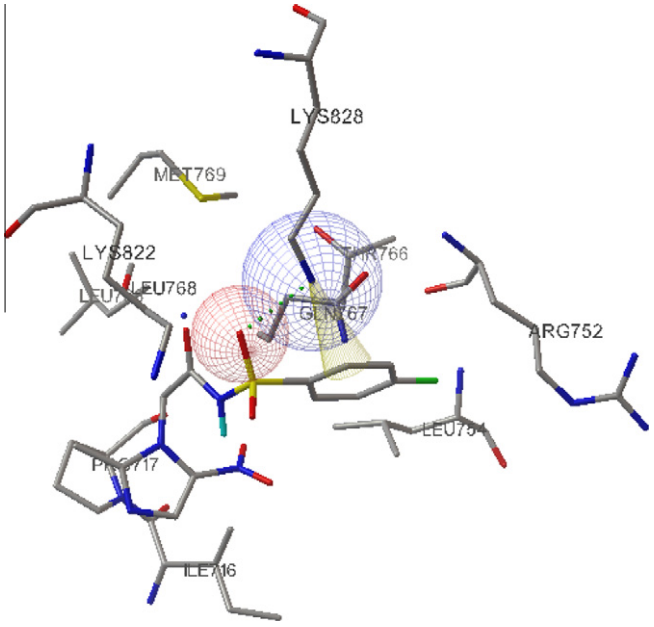

Figure 2. Binding mode of compound **12** (colored by atom: carbons: gray; oxygens: red) with EGFR enzyme (entry 1M17 in the Protein Data Bank). The dotted lines show the hydrogen bonds and the π–cation interaction is shown as yellow column.

A549 and mouse melanoma cells B16-F10, in both of which EGFR are overexpressed. As shown in Table 3, compounds **12** and **22**, which had potent inhibitory activity of EGFR showed high antiproliferative activities (IC_{50} = 1.26 and 5.64 μg/mL for A549 and IC_{50} = 0.35 and 4.23 μg/mL for B16-F10), indicating that these benzenesulfonamide derivatives were potent anticancer agents as inhibitor of EGFR. In particular, compound **12** has shown significant inhibitory activity in tumor growth and displayed favorable EGFR inhibitory activity.

To gain better understanding on the potency of the 10 compounds and guide further SAR studies, we proceeded to examine the interaction of these compounds with EGFR (PDB code: 1M17) by molecular docking, which was performed by simulation of the 10 compounds into the ATP binding site in EGFR. All docking runs were applied the Lamarckian genetic algorithm of Auto-Dock 4.0.[20] The binding model of compound **12** and EGFR is depicted in Figure 2. The amino acid residues which had interaction with EGFR were labeled. In the binding mode, compound **12** was nicely bound to the ATP binding site of EGFR hydrophobic interaction and binding was stabilized by a hydrogen bond and a π–cation interaction.

The predicted binding free energy that includes the intermolecular energy and torsional free energy was used as the criterion for ranking. The estimated free energy of other compounds (**10**–**14** and **20**–**24**) were ranging from −14.14 to −7.95 kcal/mol. The selected pose of **12** had an estimated binding free energy of −14.14 kcal/mol (binding free energy of control compound, erlotinib is −8.83 kcal/mol). The oxygen atom of the sulfonamide system formed one hydrogen bond with the amino hydrogen of LYS828 (bond length: LYS828 N–H···O = 2.744 Å; bond angle: LYS828 N–H···O = 130.98°). This residue (LYS828) was also found to be involved in the binding of other EGFR inhibitors.[4] The amino hydrogen of LYS828 was also formed a π–cation interaction with the benzene ring of compound **12**, which enhanced the binding action between receptor EGFR and ligand compound **12**. The electron donating substituent amino –NH_2 strengthen the π–cation binding and the results indicated that it was primarily due to direct through-space interaction between the substituent and the cation.[21]

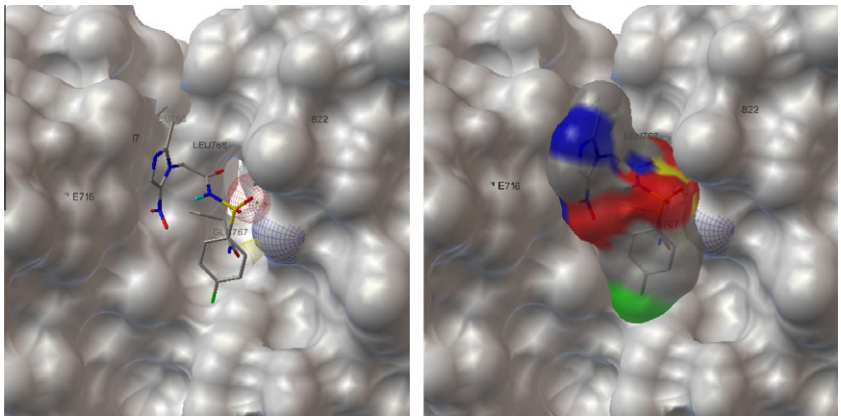

Figure 3A. 3D model of the interaction between compound **12** and the ATP binding site. The protein is represented by molecular surface. Left: **12** is depicted by sticks and balls. Right: **12** is depicted by molecular surface, sticks and balls.

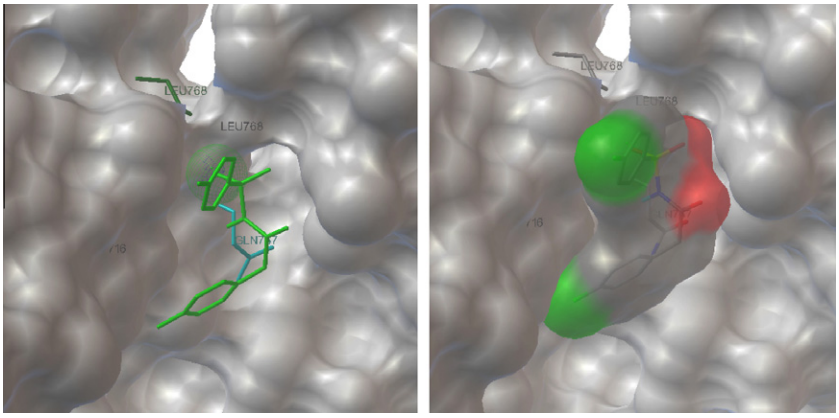

Figure 3B. 3D model of the interaction between compound **22** and the ATP binding site. The protein is represented by molecular surface. Left: **22** is depicted by sticks and balls. Right: **22** is depicted by molecular surface, sticks and balls.

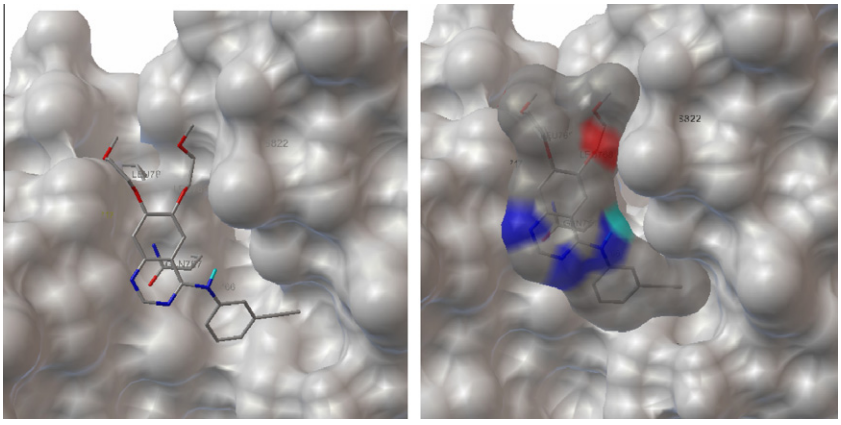

Figure 3C. 3D model of the interaction between erlotinib and the ATP binding site. The protein is represented by molecular surface. Left: erlotinib is depicted by sticks and balls. Right: erlotinib is depicted by molecular surface, sticks and balls.

3D model of the interaction between compound **12** or **22** and the ATP binding site was depicted in Figure 3A and 3B. The model was similar with the models between erlotinib and the ATP binding site (Fig. 3C). Comparing these models, it was found that the hydrophobic pockets of ATP binding site were occupied by these compounds, and the difference was the arrangement on the enzyme surface.

Meanwhile, we chose **22** as the positive control in the docking procedure. In Figure 3B, it was found that there was only one hydrogen bond in the binding pocket. The sulfonamide oxygen atom of compound **22** formed one hydrogen bond with the amino hydrogen of LEU768 (bond length: LEU768 N–H···O = 2.741 Å; bond angle: LEU768 N–H···O = 148.07°). Furthermore, in the comparison to Erlotinib's binding mode (Fig. 3C), the formation of hydrogen bond with LYS828 and the π–cation interaction seemed significant for **12** and the binding energy was up to −14.14 kcal/mol, better than −8.83 kcal/mol from the optimal binding conformation of Erlotinib (Fig. 3C). This molecular docking result, along with the biological assay data, suggesting that compound **12** is a potential inhibitor of EGFR.

3. Conclusion

In this paper, a series of novel EGFR inhibitors (**10–14** and **20–44**) bearing metronidazole (or substituted phenylacetic acid skeleton) and benzenesulfonamide moiety had been synthesized and their biological activities were evaluated. These compounds exhibited potent EGFR and HER-2 inhibitory activities and antiproliferative activities against A549 cell lines and B16-F10 cell lines. Compound **12** showed the most potent EGFR inhibition activities (IC_{50} = 0.39 μM for EGFR and IC_{50} = 1.53 μM for HER-2) and anticancer activities (IC_{50} = 1.26 μg/mL for A549 and IC_{50} = 0.35 μg/mL for B16-F10). Molecular docking was further performed to study the inhibitor-EGFR protein interactions. After analysis of the binding model of compound **12** with EGFR, it was found that a hydrogen bond and a π–cation interaction with the protein residues in the ATP binding site might play a crucial role in its EGFR inhibition and antiproliferative activities. Among these compounds, it could be concluded that compound **12** had been demonstrated to show significant EGFR and tumor growth inhibitory activity as a potential anticancer agent. The result of this work might be helpful for the design and synthesis of EGFR inhibitors with stronger activities.

4. Experiments

4.1. Materials and measurements

All chemicals and reagents used in current study were of analytical grade. All the 1H NMR spectra were recorded on a Bruker DPX 300 model Spectrometer in $CDCl_3$ or DMSO-d_6 and chemical shifts were reported in ppm (δ). ESI-MS spectra were recorded on a Mariner System 5304 Mass spectrometer. Elemental analyses were performed on a CHN-O-Rapid instrument. TLC was performed on

the glass-backed silica gel sheets (Silica Gel 60 GF254) and visualized in UV light (254 nm). Column chromatography was performed using silica gel (200–300 mesh) eluting with ethyl acetate and petroleum ether.

4.2. General procedure for synthesis of metronidazole–sulfonamide derivatives (10–14)

Compound **4** was synthesized from metronidazole (**3**) according the modified procedure of Javad et al.[19] To a stirring suspension of metronidazole (**3**, 8.55 g, 0.05 mol) in water (20 mL) at room temperature was added a solution of 14.25 g of sodium dichromate in water (69 mL) followed by drop wise addition of sulfuric acid (28.5 mL 50%). The mixture was stirred overnight. The reaction mixture was carefully neutralized with 4 N NaOH aqueous solution (250 mL). It was extracted with ethyl acetate/THF (1:1, 4 × 30 mL). The combined organic layer was washed with brine (100 mL), dried under Na_2SO_4 and evaporated under reduced pressure. The crude residue was recrystallized from CH_2Cl_2 to give compound **4**.

To a round-bottom flask (500 mL) that contained a solution of aryl sulfonamide (6 mmol), 4-dimethyaminopyridine (DMAP, 13 mmol), and 1-[3-(dimethyamino)-propyl]-3-ethylcarbodiimide hydrochloride (EDCI, 13 mmol) in CH_2Cl_2 (150 mL) was added the synthesized compound **4** (6 mmol) at room temperature. The resulting mixture was stirred at room temperature for 12 h, then cooled to 5 °C, and acidified to pH 1 with addition of HCl aqueous solution (10%), which was followed by extraction with CH_2Cl_2/MeOH (9:1, 3 × 100 mL). The combined organic layers were washed with H_2O and brine, dried over using Na_2SO_4, and concentrated in vacuo. The residue was subjected to silica gel chromatography or crystallization if necessary to afford the compounds (**11**–**14**) (Scheme 1).

4.2.1. 2-(2-Methyl-5-nitro-1*H*-imidazol-1-yl)-*N*-(phenylsulfonyl)acetamide (10)

Yield 82%; mp 262 °C. ^{1}H NMR (300 Hz, DMSO-d_6): δ 2.31 (s, 3H); 5.08 (s, 2H); 7.59–7.64 (t, J = 7.41 Hz, 2H); 7.69–7.74 (t, J = 7.5 Hz, 1H); 7.89–7.92 (t, J = 4.2 Hz, 2H); 7.98 (s, 1H) ppm. ESI-MS: 325.31 ($C_{12}H_{13}N4O_5S$, $[M+H]^+$). Anal. Calcd for $C_{12}H_{12}N_4O_5S$: C, 44.44; H, 3.73; N, 17.28. Found: C, 44.29; H, 3.79; N, 17.32.

4.2.2. 2-(2-Methyl-5-nitro-1*H*-imidazol-1-yl)-*N*-tosylacetamide (11)

Yield 85%; mp 246 °C. ^{1}H NMR (300 Hz, DMSO-d_6): δ 2.51 (s, 3H); 5.07 (s, 2H); 7.41(d, J = 8.22 Hz, 2H); 7.78 (d, J = 8.22 Hz, 2H); 7.99 (s, 1H). ESI-MS: 339.07 ($C_{13}H_{15}N_4O_5S$, $[M+H]^+$). Anal. Calcd for $C_{13}H_{14}N_4O_5S$: C, 46.15; H, 4.17; N, 16.56; Found: C, 46.25; H, 4.23; N, 16.45.

4.2.3. *N*-(4-Fluorophenylsulfonyl)-2-(2-methyl-5-nitro-1*H*-imidazol-1-yl) acetamide (12)

Yield 84%; mp 232–234 °C. ^{1}H NMR (300 Hz, DMSO-d_6): δ 2.32 (s, 3H); 5.07 (s, 2H); 7.43–7.49 (t, J = 8.77 Hz, 2H); 7.95–7.99 (m, 3H). ESI-MS: 343.04 ($C_{12}H_{12}FN_4O_5S$, $[M+H]^+$). Anal. Calcd for $C_{12}H_{11}FN_4O_5S$: C, 42.11; H, 3.24; N, 16.37. Found: C, 42.23; H, 3.12; N, 16.49.

4.2.4. *N*-(4-Chlorophenylsulfonyl)-2-(2-methyl-5-nitro-1*H*-imidazol-1-yl) acetamide (13)

Yield 81%; mp 252 °C. ^{1}H NMR (300 Hz, DMSO-d_6): δ 2.32 (s, 3H); 5.06 (s, 2H); 7.73 (d, J = 8.61 Hz, 2H); 7.89 (d, J = 6.78 Hz, 2H); 7.99(s, 1H). ESI-MS: 359.01 ($C_{12}H_{12}ClN_4O_5S$, $[M+H]^+$). Anal. Calcd for $C_{12}H_{11}ClN_4O_5S$: C, 40.17; H, 3.09; N, 15.62. Found: C, 40.23; H, 3.29; N, 15.45.

4.2.5. *N*-(4-Bromophenylsulfonyl)-2-(2-methyl-5-nitro-1*H*-imidazol-1-yl) acetamide (14)

Yield 81%; mp 275 °C. ^{1}H NMR (300 Hz, DMSO-d_6): δ 2.33 (s, 3H); 5.06 (s, 2H); 7.71 (d, J = 8.58 Hz, 2H); 7.90 (d, J = 6.79 Hz, 2H); 7.96 (s, 1H). ESI-MS: 402.96 (C12H12BrN4O5S, $[M+H]^+$). Anal. Calcd for $C_{12}H_{11}BrN_4O_5S$: C, 35.75; H, 2.75; N, 13.90. Found: C, 35.64; H, 2.73; N, 13.95.

4.3. General procedure for synthesis of phenylacetyl bezenesulfonamides (20–44)

To a round-bottom flask (500 mL) that contained a solution of aryl sulfonamide (6 mmol), 4-dimethyaminopyridine (DMAP, 13 mmol), and 1-[3-(dimethyamino)-propyl]-3-ethylcarbodiimide hydrochloride (EDCI, 13 mmol) in CH_2Cl_2 (150 mL) was added the synthesized phenylacetic acid (6 mmol) at room temperature. The resulting mixture was stirred at room temperature for 12 h, then cooled to 5 °C, and acidified to pH 1 with addition of HCl aqueous solution (10%), which was followed by extraction with CH_2Cl_2/MeOH (9:1, 3 × 100 mL). The combined organic layers were washed with H_2O and brine, dried over Na_2SO_4, and concentrated in vacuo. The residue was subjected to silica gel chromatography or crystallization if necessary to afford the compounds (**20**–**44**) (Scheme 2).

4.3.1. 2-(4-Fluorophenyl)-*N*-(phenylsulfonyl)acetamide (20)

Yield 82%; mp 115–117 °C. ^{1}H NMR (300 MHz, DMSO-d_6): δ 3.56 (s, 2H); 7.25–7.28 (m, 3H); 7.33–7.37 (m, 2H); 7.39–7.42 (m, 1H); 7.50–7.56 (m, 1H); 7.70 (d, J = 8.22 Hz, 1H); 7.97 (d, J = 8.4 Hz, 1H); 13.54 (s, 1 Hz); ESI-MS: 294.05 ($C_{14}H_{13}FNO_3S$, $[M+H]^+$). Anal. Calcd for $C_{14}H_{12}FNO_3S$: C, 57.33; H, 4.12; N, 4.78. Found: C, 57.13; H, 4.15; N, 4.75.

4.3.2. 2-(4-Fluorophenyl)-*N*-tosylacetamide (21)

Yield 82%; mp 96 °C. ^{1}H NMR (300 MHz, DMSO-d_6): δ 2.32 (s, 3H); 3.56 (s, 2H); 7.26 (d, J = 6.36, 2H); 7.34–7.37 (m, 2H); 7.50–7.55 (m, 1H); 7.70 (d, J = 8.43 Hz, 1H); 7.96 (d, J = 8.4 Hz, 1H); 13.54 (s, 1 Hz). ESI-MS: 308.07 ($C_{15}H_{15}FNO_3S$, $[M+H]^+$). Anal. Calcd for $C_{15}H_{14}FNO_3S$: C, 58.62; H, 4.59; N, 4.56. Found: C, 58.45; H, 4.55; N, 4.58.

4.3.3. 2-(4-Fluorophenyl)-*N*-(4-fluorophenylsulfonyl)acetamide (22)

Yield 82%; mp 89–90 °C. ^{1}H NMR (300 MHz, DMSO-d_6): δ 3.57 (s, 2H); 7.17 (d, J = 8.13 Hz, 2H); 7.35 (d, J = 8.83, 2H); 7.54–7.59 (d, J = 8.70 Hz, 2H); 7.90–7.94 (m, 2H); 12.45 (s, 1H). ESI-MS: 312.04 ($C_{14}H_{12}F_2NO_3S$, $[M+H]^+$). Anal. Calcd for $C_{14}H_{11}F_2NO_3S$: C, 54.01; H, 3.56; N, 4.50. Found: C, 54.21; H, 3.54; N, 4.53.

4.3.4. *N*-(4-Chlorophenylsulfonyl)-2-(4-fluorophenyl)acetamide (23)

Yield 82%; mp 102–104 °C. ^{1}H NMR (300 MHz, DMSO-d_6): δ 3.57 (s, 2H); 7.15 (d, J = 8.4 Hz, 2H); 7.34 (d, J = 8.43, 2H); 7.42–7.48 (d, J = 8.76 Hz, 2H); 7.94–7.99 (m, 2H); 12.46 (s, 1H). ESI-MS: 328.01 ($C_{14}H_{12}ClFNO_3S$, $[M+H]^+$). Anal. Calcd for $C_{14}H_{11}ClFNO_3S$: C, 51.30; H, 3.38; N, 4.27. Found: C, 51.41; H, 3.43; N, 4.25.

4.3.5. *N*-(4-Bromophenylsulfonyl)-2-(4-fluorophenyl)acetamide (24)

Yield 85%; mp 143–145 °C. ^{1}H NMR (300 MHz, DMSO-d_6): δ 3.56 (s, 2H); 7.11 (d, J = 8.22 Hz, 2H); 7.47 (d, J = 8.25 Hz, 2H); 7.78–7.85 (m, 4H); 12.46 (s, 1H). ESI-MS: 371.96 ($C_{14}H_{12}BrFNO_3S$, $[M+H]^+$). Anal. Calcd for $C_{14}H_{11}BrFNO_3S$: C, 45.18; H, 2.98; N, 3.76. Found: C, 45.29; H, 2.95; N, 3.75.

4.3.6. 2-(4-Chlorophenyl)-*N*-(phenylsulfonyl)acetamide (25)

Yield 85%; mp 125–127 °C. ^{1}H NMR(300 MHz, DMSO-d_6): 3.56 (s, 2H); 7.25–7.28 (m, 3H); 7.33–7.37 (m, 2H); 7.39–7.42 (m, 1H); 7.50–7.56 (m, 1H); 7.70 (d, J = 8.22 Hz, 1H); 7.97 (d, J = 8.4 Hz, 1H); 13.54 (s, 1 Hz); ESI-MS: 310.02 ($C_{14}H_{13}ClNO_3S$, $[M+H]^+$). Anal. Calcd for $C_{14}H_{12}ClNO_3S$: C, 54.28; H, 3.90; N, 4.52. Found: C, 54.37; H, 3.76; N, 4.83.

4.3.7. 2-(4-Chlorophenyl)-*N*-tosylacetamide (26)

Yield 82%; mp 128–130 °C. ^{1}H NMR (300 MHz, DMSO-d_6): δ 2.32 (s, 3H); 3.56 (s, 2H); 7.26 (d, J = 6.36, 2H); 7.34–7.37 (m, 2H); 7.50–7.55 (m, 1H); 7.70 (d, J = 8.43 Hz, 1H); 7.96 (d, J = 8.4 Hz, 1H); 13.54 (s, 1 Hz). ESI-MS: 324.04 ($C_{15}H_{15}ClNO_3S$, $[M+H]^+$). Anal. Calcd for $C_{15}H_{14}ClNO_3S$: C, 55.64; H, 4.36; N, 4.33. Found: C, 55.49; H, 4.45; N, 4.51.

4.3.8. 2-(4-Chlorophenyl)-*N*-(4-fluorophenylsulfonyl)acetamide (27)

Yield 80%; mp 144 °C. ^{1}H NMR (300 MHz, DMSO-d_6): δ 3.57 (s, 2H); 7.17 (d, J = 8.4 Hz, 2H); 7.34 (d, J = 8.43, 2H); 7.42–7.48 (d, J = 8.76 Hz, 2H); 7.94–7.99 (m, 2H); 12.46 (s, 1H). ESI-MS: 328.01 ($C_{14}H_{12}ClFNO_3S$, $[M+H]^+$). Anal. Calcd for $C_{14}H_{11}ClFNO_3S$: C, 51.30; H, 3.38; N, 4.27. Found: C, 52.41; H, 3.43; N, 4.25.

4.3.9. *N*-(4-Bromophenylsulfonyl)-2-(4-chlorophenyl)acetamide (29)

Yield 83%; mp 228–230 °C. ^{1}H NMR (300 MHz, DMSO-d_6): δ 3.56 (s, 2H); 7.11 (d, J = 8.22 Hz, 2H); 7.47 (d, J = 8.25 Hz, 2H); 7.78–7.85 (m, 4H); 12.46 (s, 1H). ESI-MS: 387.93 ($C_{14}H_{12}BrClNO_3S$, $[M+H]^+$). Anal. Calcd for $C_{14}H_{11}ClFNO_3S$: C, 43.26; H, 2.85; N, 3.60. Found: C,43.19; H, 2.89; N, 3.67.

4.3.10. 2-(4-Bromophenyl)-*N*-(phenylsulfonyl)acetamide (30)

Yield 85%; mp 139–140 °C. ^{1}H NMR (300 MHz, DMSO-d_6): δ 3.57 (s, 2H); 7.22 (d, J = 8.25 Hz, 2H); 7.39-.7.44 (t, J = 7.5 Hz, 1H); 7.49–7.57 (m, 4H); 7.72 (d, J = 8.22 Hz, 1H); 7.98 (d, J = 8.61 Hz, 1H); 13.52 (s, 1H). ESI-MS: 353.97 ($C_{14}H_{13}BrNO_3S$, $[M+H]^+$). Anal. Calcd for $C_{14}H_{12}BrNO_3S$: C, 47.47; H, 3.41; N, 3.95. Found: C, 47.32; H, 3.56; N, 4.09.

4.3.11. 2-(4-Bromophenyl)-*N*-tosylacetamide (31)

Yield 82%; mp 137 °C. ^{1}H NMR (300 MHz, DMSO-d_6): δ 2.32 (s, 3H); 3.56 (s, 2H); 7.22 (d, J = 5.13 Hz, 2H); 7.40–7.43 (t, J = 7.40 Hz, 1H); 7.49–7.51 (m, 2H); 7.53–7.56 (t, J = 4.58 Hz, 1H); 7.72 (d, J = 4.95 Hz, 1H); 7.98 (d, J = 5.13 Hz, 1H); 13.59 (s, 1H). ESI-MS: 367.99 ($C_{15}H_{15}BrNO_3S$, $[M+H]^+$). Anal. Calcd for $C_{15}H_{14}BrNO_3S$: C, 48.92; H, 3.83; N, 3.80. Found: C, 48.75; H, 3.96; N, 3.72.

4.3.12. 2-(4-Bromophenyl)-*N*-(4-fluorophenylsulfonyl) aceta mide (32)

Yield 83%; mp 160–161 °C. ^{1}H NMR (300 MHz, DMSO-d_6): δ 3.55 (s, 2H); 7.11 (d, J = 8.22 Hz, 2H); 7.42–7.48 (m, 4H); 7.94–7.99 (m, 2H); 12.41 (s, 1H). ESI-MS: 371.96 ($C_{14}H_{12}BrFNO_3S$, $[M+H]^+$). Anal. Calcd for $C_{14}H_{11}BrFNO_3S$: C, 45.18; H, 2.98; N, 3.76. Found: C, 45.29; H, 2.88; N, 3.84.

4.3.13. 2-(4-Bromophenyl)-*N*-(4-chlorophe nylsulfonyl) acetamide (33)

Yield 83%; mp 187–188 °C. ^{1}H NMR (300 MHz, DMSO-d_6): δ 3.57 (s, 2H); 7.17 (d, J = 8.61 Hz, 2H); 7.34 (d, J = 6.6 Hz, 2H); 7.79–7.85 (m, 4H); 12.46 (s, 1H); ESI-MS: 387.93 (C14H12BrClNO3S, $[M+H]^+$). Anal. Calcd for $C_{14}H_{11}BrClNO_3S$: C, 43.26; H, 2.85; N, 3.60. Found: C, 43.12; H, 2.83; N, 3.62%.

4.3.14. 2-(4-Bromophenyl)-*N*-(4-bromopheny lsulfonyl) acetamide (34)

Yield 81%; mp 218–221 °C. ^{1}H NMR (300 MHz, DMSO-d_6): δ 3.56 (s, 2H); 7.10 (d, J = 8.28 Hz, 2H); 7.32 (d, J = 6.54 Hz, 2H); 7.72–7.9 (m, 4H); 12.47 (s, 1H); ESI-MS: 431.88 ($C_{14}H_{12}Br_2NO_3S$, $[M+H]^+$). Anal. Calcd for $C_{14}H_{11}Br_2NO_3S$: C, 38.82; H, 2.56; N, 3.23; Found: C, 38.91; H, 2.60; N, 3.12.

4.3.15. *N*-(4-Fluorophenylsulfonyl)-2-(4-methoxy phenyl) acetamide (37)

Yield 87%; mp 130–132 °C. ^{1}H NMR (300 MHz, DMSO-d_6): δ 3.60 (s, 2H); 3.73 (s, 3H); 7.27 (d, J = 4.40, 1H); 7.28–7.34 (m, 2H); 7.39–7.42 (t, J = 4.50 Hz, 1H); 7.51–7.54 (t, J = 4.60 Hz, 1H); 7.70 (d, J = 5.11 Hz, 1H); 7.97 (d, J = 5.73 Hz, 1H); 13.01 (s, 1H). ESI-MS: 324.06 ($C_{15}H_{15}FNO_4S$, $[M+H]^+$). Anal. Calcd for $C_{15}H_{14}FNO_4S$: C, 55.72; H, 4.36; N, 4.33. Found: C, 55.34; H, 4.35; N, 4.30.

4.3.16. *N*-(4-Bromophenylsulfonyl)-2-(4-methoxyphenyl) acetamide (39)

Yield 87%; mp 172–173 °C. ^{1}H NMR (300 MHz, DMSO-d_6): δ 3.61 (s, 2H); 3.75 (s, 3H); 7.23 (d, J = 4.59, 1H); 7.30–7.36 (m, 2H); 7.40–7.43 (t, J = 4.58 Hz, 1H); 7.53–7.56 (t, J = 4.58 Hz, 1H); 7.72 (d, J = 5.13 Hz, 1H); 7.98 (d, J = 5.76 Hz, 1H); 13.59 (s, 1H). ESI-MS: 382.98 ($C_{15}H_{15}BrNO_4S$, $[M+H]^+$). Anal. Calcd for $C_{15}H_{14}BrNO_4S$: C, 46.89; H, 3.67; N, 3.65. Found: C, 46.75; H, 3.65; N, 3.66.

4.3.17. 2-(3-Bromophenyl)-*N*-(phenylsulfonyl)acetamide (40)

Yield 84%; mp 84–86 °C. ^{1}H NMR (300 MHz, DMSO-d_6): δ 3.60 (s, 2H); 7.26–7.30 (m, 3H); 7.40–7.45 (m, 2H); 7.48 (s, 1H); 7.53–7.56 (m, 1H); 7.71 (d, J = 5.13 Hz, 1H); 7.98 (d, J = 5.13 Hz, 1H); 13.58 (s, 1H). ESI-MS: 353.97 ($C_{14}H_{13}BrNO_3S$, $[M+H]^+$). Anal. Calcd for $C_{14}H_{12}BrNO_3S$: C, 47.47; H, 3.41; N, 3.95. Found: C, 47.32; H, 3.56; N, 3.87.

4.3.18. 2-(3-Bromophenyl)-*N*-tosylacetamide (41)

Yield 84%; mp 71–71 °C. ^{1}H NMR(300 MHz, DMSO-d_6): δ 2.45 (s, 3H); 3.61 (s, 2H); 7.26–7.29 (m, 2H); 7.41–7.47 (m, 2H); 7.50 (s, 1H); 7.54–7.57 (m, 1H); 7.75 (d, J = 5.10 Hz, 1H); 7.98 (d, J = 5.25 Hz, 1H); 13.58 (s, 1H). ESI-MS: 367.99 ($C_{15}H_{15}BrNO_3S$, $[M+H]^+$). Anal. Calcd for $C_{14}H_{12}BrNO_3S$: C, 48.92; H, 3.83; N, 3.80. Found: C, 48.70; H, 3.80; N, 3.82.

4.3.19. 2-(3-Bromophenyl)-*N*-(4-fluorophenylsulfonyl) acetamide (42)

Yield 84%; mp 67–69 °C. ^{1}H NMR (300 MHz, DMSO-d_6): δ 3.59 (s, 2H); 7.24–7.28 (m, 2H); 7.45–7.49 (m, 2H); 7.52 (s, 1H); 7.57–7.61 (m, 1H); 7.74 (d, J = 5.19 Hz, 1H); 7.93 (d, J = 5.70 Hz, 1H); 13.52 (s, 1H). ESI-MS: 371.96 ($C_{14}H_{12}BrFNO_3S$, $[M+H]^+$). Anal. Calcd for $C_{14}H_{11}BrFNO_3S$: C, 45.18; H, 2.98; N, 3.76. Found: C, 45.02; H, 2.95; N, 3.74.

4.3.20. 2-(3-Bromophenyl)-*N*-(4-chlorophenylsulfonyl) acetamide (43)

Yield 84%; mp 80–83 °C. ^{1}H NMR (300 MHz, DMSO-d_6): δ 3.63 (s, 2H); 7.36–7.41 (m, 2H); 7.46–7.49 (m, 2H); 7.53 (s, 1H); 7.59–7.63 (m, 1H); 7.77 (d, J = 5.20 Hz, 1H); 8.02 (d, J = 5.31 Hz, 1H); 13.73 (s, 1H). ESI-MS: 387.93 ($C_{14}H_{12}BrClNO_3S$, $[M+H]^+$). Anal. Calcd for $C_{14}H_{11}BrClNO_3S$: C, 43.26; H, 2.85; N, 3.60. Found: C, 43.32; H, 2.81; N, 3.63.

4.3.21. 2-(3-Bromophenyl)-*N*-(4-bromophenylsulfonyl) acetamide (44)

Yield 84%; mp 99–102 °C. ^{1}H NMR(300 Hz, DMSO-d_6): δ 3.62 (s, 2H); 7.40–7.44 (m, 2H); 7.52–7.56 (m, 2H); 7.64 (s, 1H); 7.73–7.78 (m, 1H); 7.82 (d, J = 5.14 Hz, 1H); 8.12 (d, J = 5.16 Hz, 1H); 14.02 (s,

1H). ESI-MS: 431.88 ($C_{14}H_{12}Br_2NO_3S$, $[M+H]^+$). Anal. Calcd for $C_{14}H_{11}Br_2NO_3S$: C, 38.82; H, 2.56; N, 3.23; Found: C, 38.19; H, 2.52; N, 3.26.

4.4. General procedure for preparation, purification of HER-2 and EGFR, and inhibitory assay

A 1.7 Kb cDNA encoded for human HER-2 cytoplasmic domain (HER-2-CD, amino acids 676–1245) and 1.6 Kb cDNA encoded for the EGFR cytoplasmic domain (EGFR-CD, amino acids 645–1186) were cloned into baculoviral expression vectors pBlueBacHis2B and pFASTBacHTc (Huakang Company, China), separately. A sequence that encodes $(His)_6$ was located at the 5′ upstream to the HER-2 and EGFR sequences. Sf-9 cells were infected for three days for protein expression. Sf-9 cell pellets were solubilized at 0 °C in a buffer at pH 7.4 containing 50 mM HEPES, 10 mM NaCl, 1% Triton, 10 μM ammonium molybdate, 100 μM sodium vanadate, 10 μg/mL aprotinin, 10 μg/mL leupeptin, 10 μg/mL pepstatin, and 16 μg/mL benzamidine HCl for 20 min followed by 20 min centrifugation. Crude extract supernatant was passed through an equilibrated Ni-NTA superflow packed column and washed with 10 mM and then 100 mM imidazole to remove nonspecifically bound material. Histidine tagged proteins were eluted with 250 and 500 mM imidazole and dialyzed against 50 mM NaCl, 20 mM HEPES, 10% glycerol, and 1 μg/mL each of aprotinin, leupeptin, and pepstatin for 2 h. The entire purification procedure was performed at 4 °C or on ice.[22]

Both EGFR and HER-2 kinase assays were set up to assess the level of autophosphorylation based on DELFIA/Time-Resolved Fluorometry. Compounds **10**–**14** and **20**–**44** were dissolved in 100% DMSO and diluted to the appropriate concentrations with 25 mM HEPES at pH 7.4. In each well, 10 μL compound was incubated with 10 μL (12.5 ng for HER-2 or 5 ng for EGFR) recombinant enzyme (1:80 dilution in 100 mM HEPES) for 10 min at room temperature. Then, 10 μL of 5 mM buffer (containing 20 mM HEPES, 2 mM $MnCl_2$, 100 μM Na_3VO_4, and 1 mM DTT) and 20 μL of 0.1 mM ATP–50 mM $MgCl_2$ were added for 1 h. Positive and negative controls were included in each plate by incubation of enzyme with or without ATP–$MgCl_2$. At the end of incubation, liquid was aspirated, and plates were washed three times with wash buffer. A 75 μL (400 ng) sample of europium labeled anti-phosphotyrosine antibody was added to each well for another 1 h of incubation. After washing, enhancement solution was added and the signal was detected by Victor (Wallac Inc.) with excitation at 340 nm and emission at 615 nm. The percentage of autophosphorylation inhibition by the compounds was calculated using the following formula: 100% − [(negative control)/(positive control − negative control)]. The IC_{50} was obtained from curves of percentage inhibition with eight concentrations of compound. As the contaminants in the enzyme preparation are fairly low, the majority of the signal detected by the anti-phosphotyrosine antibody is from EGFR or HER-2.

4.5. Antiproliferation assay

The antiproliferative activities of the prepared compounds (**10**–**14** and **20**–**24**) against A549 adenocarcinomic human alveolar basal epithelial cell line and B16-F10 mouse melanoma cell line were evaluated as described elsewhere with some modifications.[23] Target tumor cell lines were grown to log phase in RPMI 1640 medium supplemented with 10% fetal bovine serum. After diluting to 2×10^4 cells mL^{-1} with the complete medium, 100 μL of the obtained cell suspension was added to each well of 96-well culture plates. The subsequent incubation was permitted at 37 °C, 5% CO_2 atmosphere for 24 h before the cytotoxicity assessments. Tested samples at pre-set concentrations were added to six wells with erlotinib assayed as positive reference. After 48 h exposure period, 40 μL of PBS containing 2.5 mg mL^{-1} of MTT (3-(4,5-dimethylthiazol–2-yl)-2,5-diphenyltetrazolium bromide)) was added to each well. Four hours later, 100 μL extraction solution (10% SDS–5% isobutyl alcohol–0.01 M HCl) was added. After an overnight incubation at 37 °C, the optical density was measured at a wavelength of 570 nm on an ELISA microplate reader. In all experiments three replicate wells were used for each drug concentration. Each assay was carried out for at least three times. The results were summarized in Table 3.

4.6. Molecular docking modeling

Molecular docking of compounds into the 3D EGFR complex structure (1M17.pdb, downloaded from the PDB) was carried out using the AutoDock software package (version 4.0) as implemented through the graphical user interface Auto-DockTools (ADT 1.4.6).

Acknowledgments

This work was supported by Jiangsu National Science Foundation (No. BK2009239) and the Fundamental Research Funds for the Central Universities (No. 1092020804 & 1106020824).

References and notes

1. Qian, Y.; Zhang, H. J.; Zhang, H.; Xu, C.; Zhao, J.; Zhu, H. L. *Bioorg. Med. Chem.* **2010**, *18*, 4991.
2. Slamon, D. J.; Clark, G. M.; Wong, S. G.; Levin, W. J.; Ullrich, A.; McGuire, W. L. *Science* **1987**, *235*, 177.
3. Slamon, D. J.; Godolphin, W.; Jones, L. A. *Science (Washington DC)* **1989**, *244*, 707.
4. Kolibaba, K. S.; Druker, B. J. *Biochim. Biophys. Acta.* **1997**, *1333*, 217.
5. Tateishi, M.; Ishida, T.; Mitsudomi, T.; Kaneko, S.; Sugimachi, K. *Cancer Res.* **1990**, *50*, 7077.
6. Fleming, T. P.; Saxena, A.; Clark, W. C.; Robertson, J. T.; Oldfield, E. H.; Aaronson, S. A.; Ali, I. U. *Cancer Res.* **1992**, *52*, 4550.
7. Shin, D. M.; Ro, J. Y.; Hong, W. K.; Hittelamn, W. N. *Cancer Res.* **1994**, *54*, 3153.
8. Ciardiello, F.; Tortola, G. *Clin. Cancer Res.* **2001**, *7*, 2958.
9. Giglio, J.; Fernández, S.; Rey, A.; Cerecetto, H. *Bioorg. Med. Chem. Lett.* **2011**, *21*, 394.
10. Mallia, M. B.; Mathur, A.; Subramanian, S.; Banerjee, S.; Sarma, H. d.; Venkatesh, M. *Bioorg. Med. Chem. Lett.* **2005**, *15*, 3398.
11. Born, J. L.; Smith, B. R.; Harper, N.; Koch, C. *J. Biochem. Pharmacol.* **1992**, *43*, 1337.
12. Brown, J. M. *Int. J. Radiat. Oncol. Biol. Phys.* **1989**, *16*, 987.
13. Lord, E. M.; Harwell, L.; Koch, C. J. *Cancer Res.* **1993**, *53*, 5721.
14. Webster, L. T. Drugs Used in the Chemotherapy of Protozoal Infections In Gilman, A., Rall, T. W., Nies, A. S., Taylor, P., Eds.; The pharmacological basis of therapeutics; Pergamon Press: New York, 1990; pp 999–1007.
15. Alvaro, R. F.; Wislocki, P. G.; Miwa, G. T.; Lu, A. Y. *Chem. Biol. Interact.* **1992**, *82*, 21.
16. Chapman, J. D. *N. Eng. J. Med.* **1979**, *301*, 1429.
17. Lobb, K. L.; Hipskind, P. A.; Aikins, J. A.; Alvarez, E.; Cheung, Y. Y., et al *J. Med. Chem.* **2004**, *47*, 5367.
18. Corbett, T. H.; White, K.; Polin, L.; Kushner, J.; Paluch, J.; Shih, C.; Grossman, C. S. *Invest. New. Drugs.* **2003**, *21*, 33.
19. Mirzaei, J.; Amini, M.; Pirelahi1, H.; Shafiee, A. *J. Heterocycl. Chem.* **2008**, *45*, 921.
20. Huey, R.; Morris, G. M.; Olson, A. J.; Goodsell, D. S. *J. Comput. Chem.* **2007**, *28*, 1145.
21. Wheeler, S. E.; Houk, K. N. *J. Am. Chem. Soc.* **2009**, *131*, 3126.
22. Tsou, H. R.; Mamuya, N.; Johnson, B. D.; Reich, M. F.; Gruber, B. C.; Ye, F.; Nilakantan, R.; Shen, R.; Discafani, C.; DeBlanc, R.; Davis, R.; Koehn, F. E.; Greenberger, L. M.; Wang, Y. F.; Wissner, A. *J. Med. Chem.* **2001**, *44*, 2719.
23. Boumendjel, A.; Boccard, J.; Carrupt, P. A.; Nicolle, E.; Blanc, M.; Geze, A.; Choisnard, L.; Wouessidjewe, D.; Matera, E. L.; Dumontet, C. *J. Med. Chem.* **2008**, *51*, 2307.